# Phase separation, oxygen composition, and a glass transition due to freezing-in of the oxygen rearrangement in $La_2NiO_{4.094}$ single crystals

Tôru Kyômen, Masaharu Oguni,* and Kenzo Kitayama
*Department of Chemistry, Faculty of Science, Tokyo Institute of Technology, Ookayama-2, Meguro-ku, Tokyo 152, Japan*

Mitsuru Itoh
*Research Laboratory of Engineering Materials, Tokyo Institute of Technology, 4259 Nagatsuta, Midori-ku, Yokohama 227, Japan*

(Received 30 January 1995)

Heat capacities of $La_2NiO_{4.094}$ single crystal were measured in 15–400 K with an adiabatic calorimeter. Four anomalies were found, as due to a phase separation concerning the excess oxygen composition at around 285 K, a glass transition over a wide temperature range of 150–300 K, a first-order structural transition from tetragonal to orthorhombic phases at 240 K, and an antiferromagnetic phase transition at around 55 K. The glass transition appeared as giving rise to spontaneous, exothermic at low temperatures and endothermic at high temperatures, enthalpy relaxations due to irreversible equilibration processes with respect to the compositions and configurations of excess oxygen atoms. The properties of the phase separation are discussed on the basis of the relaxation rates and the heat capacity anomaly around the separation temperature.

## I. INTRODUCTION

Most high-temperature superconducting oxides and their related compounds show oxygen nonstoichiometry, and the configuration of the nonstoichiometric oxygen ions has crucial influences on the details of the crystal structure, electronic state, superconductivity, and so on. $La_2CuO_4$ and $La_2NiO_4$ crystals have the same structure of $K_2NiF_4$ type at high temperatures.[1] Both show nonstoichiometry in the oxygen composition, and the chemical formulas of the crystals are expressed by $La_2MO_{4+\delta}$ ($M$= Cu, Ni):[2] The former crystal with large $\delta$ shows superconductivity while in the latter it has not been confirmed.[3] Though both compounds show thus different properties with respect to superconductivity, some similarities between them are expected to appear in the $\delta$-$T$ phase relation and therefore in the crystal structures including the arrangements of excess oxygen ions. In view of the fact that $La_2CuO_{4+\delta}$ crystal with large $\delta$ is very difficult to prepare, combined studies on both compounds are indispensable for clarification of the static and dynamic properties of excess oxygen ions.

It is known in both compounds that the excess oxygen ions are located between adjacent LaO layers and are tetrahedrally surrounded by four La ions.[4,5] Some ordered structures of the excess oxygen ions have been suggested so far to exist. Hiroi *et al.* reported the existence of three-dimensional ordered structures in $La_2NiO_{4+\delta}$ crystals by electron diffraction (ED) and transmission electron microscopy (TEM), and indicated that the ordered structures had the $\delta$ values equal to $1/(2n)$ with $n$ as integers.[6] Tranquada *et al.*, on the other hand, suggested one-dimensional ordering similar to the staging of intercalates in graphite on the basis of the obtained superlattice reflections by a neutron diffraction technique.[7] These are understood to indicate that at high temperatures the excess oxygen ions are arranged homogeneously in a disordered way among the whole accessible sites, while that at low temperatures, if the $\delta$ is far from and in between the values expected from the favorably ordered structures, there occurs a phase separation into two regions with different oxygen compositions. In fact, the latter group proposed that crystals with $0.07 < \delta < 0.10$ showed phase separations between the regions of stage-2 and stage-3 structures with $\delta \sim 0.105$ and $\delta \sim 0.067$, respectively. A phase separation concerning the excess oxygen ions has been also discussed to occur in $La_2CuO_{4+\delta}$.[8] Considering, for example, that the above two types of ordering of excess oxygen ions lead to different $\delta$-$T$ phase relations, unambiguous determination of the phase relations for both the compounds is primarily important for making further progress in the understanding of the structures and properties of crystals.

$La_2CuO_{4+\delta}$ ($0.01 < \delta < 0.04$) and $La_2NiO_{4+\delta}$ ($0.07 < \delta < 0.10$) crystals have been discussed to show the phase separations proceeding in the temperature region of 270–290 K.[2,7,8] We previously measured and reported the heat capacities of $La_2CuO_{4+\delta}$ ($\delta$ = 0.011 and 0.035):[9,10] The results indicated that there occurred no phase separation in the oxygen composition below 310 K, but instead three phase transitions of the displacive type occurred; a second-order transition at around 287 K and 295 K, respectively, a Martensitic one around 270 K, and a first-order one at around 220 K. The second transition takes place over a relatively wide temperature range, and thermal annealing below the range enhances the growth of crystallite grains. The third transition from high- to low-temperature phases proceeds through the processes of crystal nucleation and crystal growth so that the progress of the processes will require a long annealing below the transition temperature. This understanding is reasonable considering that the phase separation

 

in the $La_2NiO_{4+\delta}$ system with $0.01 < \delta < 0.06$ has been reported by many groups to take place above room temperature.[11–13] Research groups in the above literature have misunderstood the annealing effects of the Martensitic transition and of the first-order transition as due to the sluggish progress of oxygen diffusion processes in the phase separation. The phase separation discussed so far in $La_2NiO_{4+\delta}$ ($0.07 < \delta < 0.10$) should be thus examined as well by high-precision calorimetry since progress in the order-disorder process of excess oxygen ions over a very long distance gives rise to appreciable changes in the static and kinetic aspects of thermal properties. The examination is attractive also in that such a precise calorimetry has not been applied to phase separation in any system.

In the present study, the heat capacities of a $La_2NiO_{4.094}$ single crystal were measured with a high-precision adiabatic calorimeter. For help in understanding the implication of the results, how the enthalpy relaxation due to freezing-in of the phase separation should be observed calorimetrically, is described in Sec. II. The calorimetric results are given in Sec. IV A. The phase separation properties in the present crystal are discussed in Sec. IV B on the basis of heat capacity anomalies and the rates of temperature drifts (of a calorimeter cell) originating from the relevant enthalpy relaxations.

## II. GLASS TRANSITION PHENOMENON DUE TO FREEZING-IN OF THE DIFFUSION PROCESS OF EXCESS OXYGEN IONS

Diffusion of excess oxygen ions over a long distance takes place in the process of phase separation with respect to the oxygen composition. The diffusion proceeds as a classical process by surmounting a certain potential barrier $\Delta\varepsilon_a$, as shown in Fig. 1. The diffusion frequency for a single-jump process is then expressed by

$$f_1 = f_0 \exp(-\Delta\varepsilon_a/RT) , \quad (1)$$

where $f_0$ is the frequency of the trial for surmounting the barrier $\Delta\varepsilon_a$, and therefore for jumping to a neighboring site, and $R$ is gas constant. The $f_0$ should be related to the frequency of the translational vibration of the oxygen ion, and is expected to be of the order of $\sim 10^{13}$ Hz. It is convenient to transform the expression into the following form of the characteristic relaxation time:

$$\tau_1 = \tau_0 \exp(\Delta\varepsilon_a/RT) , \quad (2)$$

where the preexponential factor $\tau_0$ is given by $1/(2\pi f_0)$ and is assumed for the present to be $10^{-14}$ s, as described previously to be reasonable.[14] The reason is that the relaxation process due to oxygen diffusion is followed in the time domain in the present work. As the temperature of the system decreases the relaxation time becomes long, and when the time becomes longer than the experimental time scale $10^2$–$10^6$ s in the present work, the configuration of excess oxygen ions is frozen in. Such a freezing-in phenomenon is called a glass transition, and the transition temperature $T_g$ is often defined as the temperature at which the relaxation time becomes $10^3$ s.[15] When the relaxation times for any processes are in the range of $10^2$–$10^6$ s, spontaneous enthalpy relaxations are observed on account of the crossing between the time scale of the diffusion process of excess oxygen ions and the calorimetry.

The diffusion of excess oxygen ions in the phase separation takes place over a long distance through surmounting plural barriers. Then, two typical cases can be considered for the jump processes as shown in Fig. 1. In case (a), two oxygen ions located initially at sites 2 and 1 move to sites 3 and 2, respectively, in turn. The relaxation time for that would be expressed by

$$\tau_2(\mathrm{a}) = 2\tau_0 \exp(\Delta\varepsilon_a/RT). \quad (3)$$

In case (b), on the other hand, the two oxygen ions located at the sites 2 and 1 move simultaneously. The relaxation time would be then expressed by

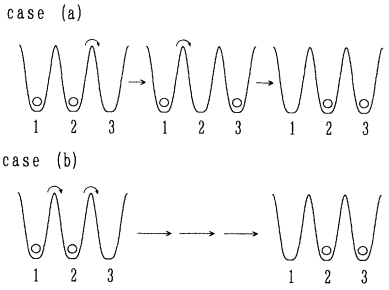


FIG. 1. A diagram showing two possible diffusion processes of excess oxygen ions: (a) two oxygen ions located at sites 2 and 1 move to 3 and 2, respectively, in turn; (b) the two oxygen ions move simultaneously.

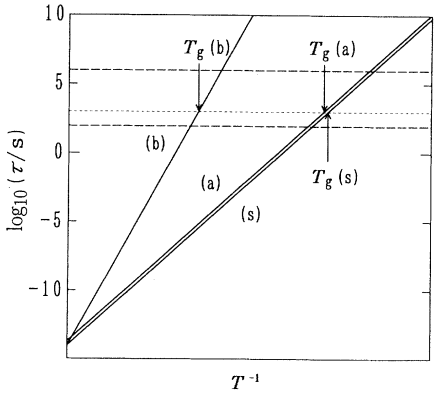


FIG. 2. Arrhenius plots of relaxation times: line ($s$), a single-step process; line (a), the process corresponding to case (a) in Fig. 1; line (b), the process corresponding to case (b) in Fig. 1. Two horizontal dashed lines represent the boundaries of the range of experimental time scale, $10^2$–$10^6$ s, by a precise adiabatic calorimetry. $T_g$'s denote the glass transition temperatures at which the relaxation times of the respective processes become $10^3$ s. See text for details.

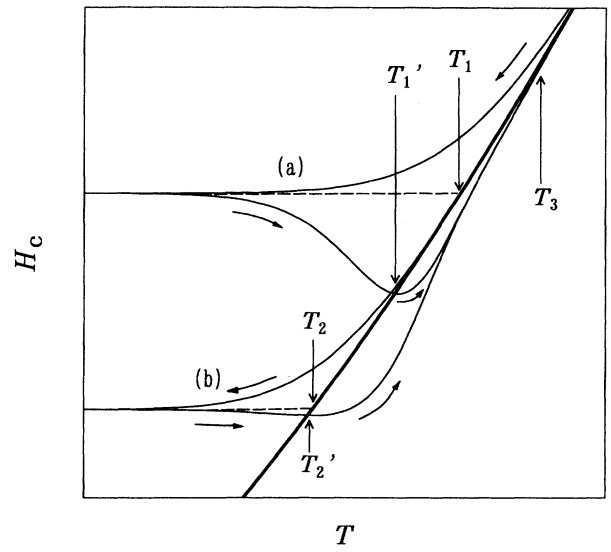


FIG. 3. Schematic configurational enthalpy vs temperature relation in a glass transition temperature region: (a) rapidly precooled sample, (b) slowly precooled sample. A thick solid line stands for the equilibrium configurational enthalpy, and thin solid lines for the paths along which the sample, when cooled and heated continuously, follows.

$$\tau_2(\mathrm{b}) = \tau_0 \exp(2\Delta\varepsilon_a/RT). \tag{4}$$

Figure 2 shows the temperature dependences of the relaxation times on the assumption that a solid line ($s$) stands for the dependence for the single-jump process given by Eq. (2). The two relaxation times of Eqs. (3) and (4) are represented by straight lines (a) and (b), respectively: The former is much shorter than the latter except at very high temperatures, and process (a) dominates overwhelmingly the diffusion of excess oxygen ions. If any oxygen ion undertakes jumps of $n$ steps in a certain diffusion process, the relaxation time would thus be written as

$$\tau_n = n\tau_0 \exp(\Delta\varepsilon_a/RT). \tag{5}$$

Here the $\Delta\varepsilon_a$ is supposed to be more or less constant for all the jump processes within the crystal.

In the real process as shown in Fig. 1(a), the diffusion in the backward direction takes place at the rate of the same order in magnitude as in the forward direction. The effective diffusion distance $l$ would be then estimated, on consideration of the random walk problem, to be on the order of $\sqrt{n}\,a$,[16] where $a$ corresponds to the jump distance of a single step.

The present calorimetry is carried out in the intermittent heating way under adiabatic conditions: The initial temperature $T_i$ is rated, for example, for 13 min, some known quantity of electrical energy, $\Delta E$, is supplied into a calorimeter cell loaded with the sample, and again the final temperature $T_f$ is rated for 13 min. The gross heat capacity of the cell is evaluated to be $\Delta E/(T_f - T_i)$ at $T_{\mathrm{av}} = (T_f + T_i)/2$. The latter temperature rating serves as the former rating in the next set of heat capacity measurements. If any spontaneous heat evolution or absorption effect appears in the sample, it is detected as a spontaneous temperature rise or fall, respectively, of the cell in the above rating periods. Figure 3 shows a diagram illustrating how the enthalpy relaxations are observed in the glass transition region, where only the situation with $n = 1$ is considered: The upper-right to lower-left thick solid lines represent the equilibrium enthalpy concerning the configurational degree of freedom of oxygen ions. When the sample is precooled rapidly, the oxygen ions are arrested in the configurational state corresponding to a relatively high temperature such as $T_1$. As the temperature increases in the course of heat capacity measurements, the configurational enthalpy starts to relax appreciably toward the equilibrium value at around the temperature at which the relaxation time becomes $10^6$–$10^7$ s. The rates of exothermic relaxations first observed become large with reduction in the relaxation times, and then become small as the configurational enthalpy approaches the equilibrium value. After crossing of the configurational enthalpy with the equilibrium line at $T_1'$, endothermic relaxations appear until the relaxation time becomes shorter than $\sim 10^2$ s at high temperatures such as $T_3$. When the sample is precooled slowly or is annealed for a long time at low temperatures around $T_2$, on the other hand, the configurational enthalpy of the sample is brought to a very low value corresponding, for example, to $T_2$ in the figure. As the temperature increases for measurements, a small exothermic effect starts to appear at around the temperature at which the relaxation time becomes $\sim 10^6$ s. A following endothermic effect starts to appear at $T_2'$ which is definitely lower than the $T_1'$ in the above case of a rapidly precooled sample, and is considerably large compared with that in the rapidly precooled case.

In the real calorimetry of the process of phase separation in the oxygen composition, the number $n$ of jump steps ranges from 1 to $10^7$ after the present result described later. Thus there always exists a wide distribution in the relaxation times expressed in Eq. (5), and the temperature dependence of the relaxation rates becomes impossible to be analyzed quantitatively. The relaxation effect observed in the low-temperature limit would be due only to the process of a single step, $n$=1, and therefore the kinetic parameters for the single-step process would be estimated from the temperature region in which the enthalpy relaxation has started to be observed on heating.

## III. EXPERIMENTAL DETAILS

Appropriate amounts of $La_2O_3$ (99.9% purity) and NiO (99.9% purity) powders were mixed, dried, and calcined in air at 1250 °C several times with intermittent mixing. The calcined powder was used as a starting material for the growth of a $La_2NiO_{4+\delta}$ single crystal. A $La_2NiO_{4+\delta}$ single crystal was grown with the same procedure as the $La_2CuO_{4+\delta}$ single crystal described

previously.[9] The amount of the mean excess oxygen content was adjusted through a high-temperature treatment at 1200 °C under an atmosphere of controlled oxygen-gas pressure.[17] The valence of nickel was determined by the iodometric titration technique and the excess oxygen content was calculated from this value with an uncertainty of about ±0.003. Heat capacities of the sample were measured in 13–400 K by an intermittent heating method under adiabatic conditions using a high-precision adiabatic calorimeter.[18] The details of the method were described in a previous paper.[10] The temperature rating after each energy supply during the measurements was carried out for 120 min in the region of 230–300 K and for 13 min otherwise.

The mass of the sample used was weighed to be 14.509 g (≙0.036 092 mol). The imprecision and the inaccuracy of the measurements with the apparatus were estimated previously to be within ±0.06% and ±0.3%, respectively.[18]

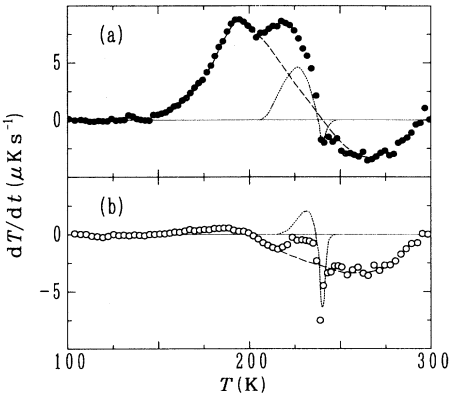


FIG. 5. Spontaneous temperature drift rates obtained during two series of measurements by the intermittent heating method: (a) rapidly precooled sample, (b) slowly precooled sample. See text for details.

## IV. RESULTS AND DISCUSSION

### A. Heat capacities and spontaneous heat evolution and absorption effects

Figure 4 shows the experimental heat capacities of a $La_2NiO_{4.094}$ single crystal. Three heat capacity anomalies were found: An anomaly around 285 K is due to a phase separation described in detail below, an anomaly at 240 K is due to a first-order phase transition from tetragonal to orthorhombic structures in the oxygen-poor region according to the literature,[7,19] and an anomaly around 55 K is considered to be due to an antiferromagnetic phase transition according to the literature.[11,20] The entropy of transition at 240 K was estimated to be of the order of 0.2 J K$^{-1}$ mol$^{-1}$. Whether the transition does or does not involve an order-disorder process of excess oxygen ions in the region is not clear only with the value.

Figures 5(a) and 5(b) show spontaneous temperature drift rates observed in the temperature range of 100–310 K for the samples precooled rapidly at 20 K min$^{-1}$ and slowly at 20 mK min$^{-1}$, respectively, from 300 K. The rates were taken as the values at 10 min after each energy supply in each series of heat capacity measurements. The former rapidly precooled sample exhibited first an exothermic effect starting at around 140–150 K and having two peaks at around 195 K and 220 K, in succession, a small endothermic shoulder at around 240 K, and a sluggish heat absorption effect over a temperature range of 240–300 K. The small endothermic effect at 240 K is definitely due to the first-order phase transition. The detailed thermal pretreatments taken in preparation of the latter slowly precooled sample are as follows: First, the sample was annealed at 250 K for 27 h after rapid cooling from 330 K, and then annealed at 220 K for 24 h after precooling to 165 K for enhancement of the nucleation of the low-temperature orthorhombic phase. After this, the sample was slowly cooled at 20 mK min$^{-1}$ from 220 K to 144 K, and then cooled rapidly down to 100 K. This slowly precooled sample showed in the series of measurements a small heat evolution effect starting at around 150–160 K, in succession, a heat absorption effect in the temperature range of 200–230 K, then a sharp endothermic peak at around 240 K, and finally the same sluggish heat absorption effect in the temperature range of 240–300 K as the rapidly precooled sample showed.

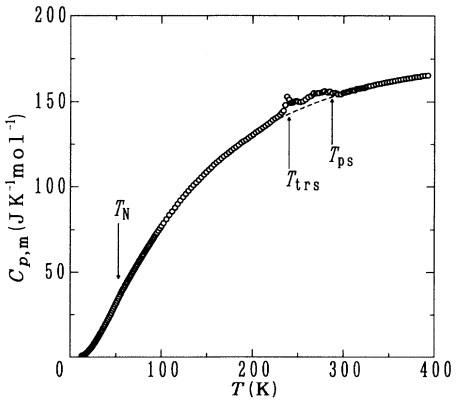


FIG. 4. Heat capacities of a $La_2NiO_{4.094}$ single crystal.

The above complicated heat evolution and absorption effects are understood as being composed of two kinds of contributions: One is concerned with the phase transition at 240 K, as shown by dotted lines. Since the transition is of the first-order type, it proceeds with the processes of new-phase nucleation and growth, and the progress of the processes often takes a long time. As the temperature of the respective samples is increased, the high-temperature tetragonal to low-temperature orthorhombic phase transition appears above 200 K and up to around 235 K. Since the slowly precooled sample was annealed at 220 K for 24 h to enhance the transition in advance, the heat evolution effect during the heat capacity measurements is smaller in the sample than in the rapidly precooled sample. The heat absorption effect, attributed to the low-temperature orthorhombic to high-temperature tetragonal phase transition, is oppositely larger in the slowly precooled sample, as is quite reasonable because the larger fraction of

the oxygen-poor region has been transformed to the low-temperature phase in the sample than in the rapidly precooled sample. The other contribution is concerned with the phase separation in the excess oxygen composition, as shown by dashed lines.

### B. Phase separation concerning the excess oxygen composition and the associated glass transition

As seen in Figs. 5(a) and 5(b), while the temperature regions in which spontaneous heat evolution and absorption effects concerning the phase transitions appeared were hardly influenced by the annealing or different precooling rates, those concerning the phase separation were influenced remarkably: The temperature of turnover from the low-temperature exothermic to high-temperature endothermic drifts changed from around 230 K for the rapidly precooled sample to around 200 K for the slowly precooled one. The systematic change is characteristic of a glass transition, and the very wide temperature regions in which the drifts are observed indicate that the glass transition is due to the freezing-in of the long-distance diffusion processes of excess oxygen ions, as described in detail in Sec. II. Further, the turnover from the exothermic to endothermic drifts was brought about by the temperature increase of a few kelvin in the series of measurements, as shown in Fig. 5(b) at around 200 K. This indicates that at least one of two phases separated in the sample changes its equilibrium excess-oxygen composition $\delta$ even at 200 K and therefore the volume fractions of the two phases vary with temperature. The situation is schematically illustrated in Fig. 6; the arrows (a) represent the exothermic process proceeding in the direction of increasing the difference between the $\delta$ values of the two phases while the arrows (b) represent the endothermic one proceeding in the opposite direction, and the turnover means that the equilibrium $\delta$ values of the two phases change appreciably with an increase of a few kelvin. It follows from this consideration that the phase separation line has, to some extent, a parabolic shape of upward convex, as depicted exaggeratedly in Fig. 6. Considering that the shape is a little different from that given in the literature,[7] determination of the detailed $\delta$-$T$ phase relation seems to require more and precise experimental researches.

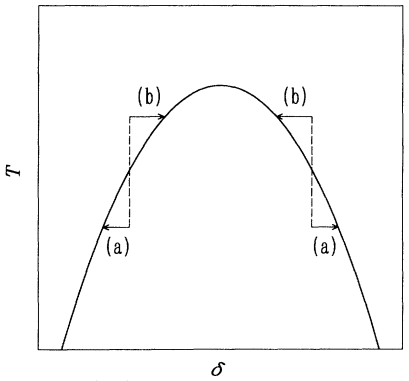


FIG. 6. Schematic diagram illustrating the feature of $\delta$-$T$ phase relation observed around 200 K: (a) the exothermic relaxation process in which the difference between the $\delta$ values of two phases increases, (b) the endothermic relaxation process in which the difference decreases. Dashed lines stand for a temperature rise due to some energy supply into the calorimeter cell.

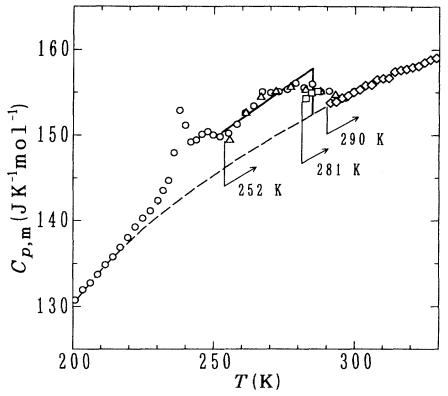


FIG. 7. Heat capacities in the temperature range of 200–330 K on an enlarged scale: ○, slowly precooled sample to 144 K; △, sample precooled to 252 K from 330 K and annealed there for 17 h; □, precooled to 281 K and annealed there for 13 h; ◇, precooled to 290 K and annealed there for 45 min. A dashed line represents the base line for the anomalies, and a thick solid line represents the equilibrium heat capacity curve supposed as including the contribution from the phase separation.

The phase separation temperature at $\delta = 0.094$ is expected from the end point of the spontaneous heat absorption in Fig. 5 to lie at around 280–290 K. Figure 7 shows the heat capacity anomalies in the temperature range of 200–330 K on an enlarged scale. Circles represent the values of the slowly precooled sample described above, and a dashed line stands for the base line expected in the case where no phase transition or phase separation take place. Triangles, squares, and diamonds represent the values of the samples precooled down to 252 K, 281 K, and 290 K, respectively, from 330 K, and annealed at the respective precooling temperatures for 17 h, 13 h,

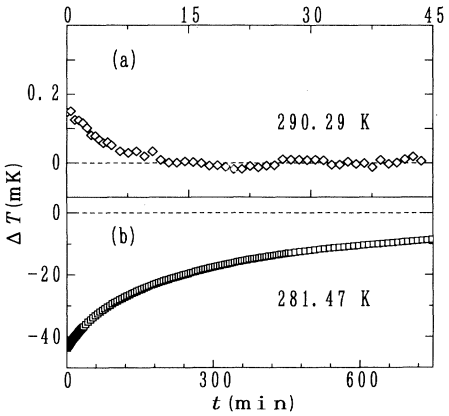


FIG. 8. Temperature drifts followed at around 290 K (a) and 281 K (b), immediately after the rapid cooling from 330 K.

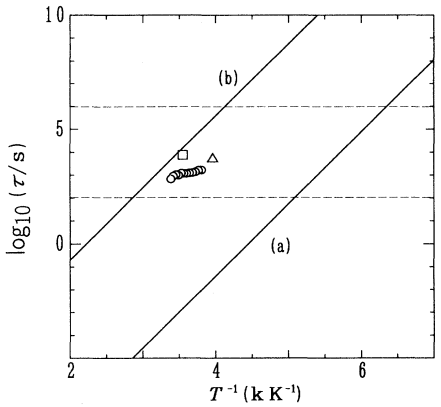


FIG. 9. Relaxation times obtained by fitting an exponential function to the relaxation data: ○, fitted to the data obtained during a series of heat capacity measurements for the slowly precooled sample; △ and □, fitted to the data at 252 K and 281 K, respectively, immediately after the rapid cooling from 330 K; line (a), Arrhenius equation (2) with $\tau_0 = 10^{-14}$ s and $\Delta\varepsilon_a$ = 55–60 kJ mol$^{-1}$; line (b), Arrhenius equation (5) with $n = 10^7$ and the same values of $\tau_0$ and $\Delta\varepsilon_a$ as in (a). Two dashed lines represent the probable limits of the time scale for the calorimetric observation of enthalpy relaxations.

and 45 min, respectively, in advance. Four sets of data are in reasonable agreement. Figures 8(a) and 8(b) show the temperature drift curves obtained just after the rapid cooling from 330 K to 290 K and to 281 K, respectively. No heat evolution appears at 290 K, but it does at 281 K. Thus the phase separation temperature at $\delta = 0.094$ was determined, taking into consideration the heat capacity curve in Fig. 7, to be $T_{ps} \approx 285$ K.

The thick solid line in Fig. 7 represents the supposed equilibrium curve of the heat capacity. The heat capacity jump at 285 K amounts to 5–6 J K$^{-1}$ mol$^{-1}$ in $La_2NiO_{4.094}$. The order of magnitude for the phase separation entropy would be estimated by assuming the heat capacity contribution $c$, approximated by $c = aT$, where $a$ is a constant. The estimation yields the value of $\sim R\ln 2$ in units of 1 mol of $La_2NiO_{4.094}$. Conversion of the entropy to the value in units of 1 mol of excess oxygen ions results in $\sim 10R\ln 2$ in the order of magnitude. This is quite a large value as is consistent with the interpretation that the anomaly at 285 K is due to the phase separation concerned with the composition and therefore the rearrangement of excess oxygen ions.

Figure 9 shows Arrhenius plots of the relaxation times estimated from the enthalpy relaxation drifts associated with the glass transition. The kinetic parameters for the single-step process may be estimated from the relaxation data at low temperatures. In view of the fact that the exothermic drift starts to be observed at around 150 K, the relaxation time for the process is of the order of magnitude of $10^6$–$10^7$ s there. The straight line (a) represents the temperature dependence of the relaxation times for the process according to the Arrhenius equation (2) with $\tau_0 = 10^{-14}$ s. $\Delta\varepsilon_a$ for the single-jump process is estimated from the slope of line (a) to be 55–60 kJ mol$^{-1}$.

The maximum number of jumps, in the present case, of oxygen ions associated with the phase separation, on the other hand, may be estimated from the relaxation data at high temperatures. Circles in the figure stand for the relaxation times evaluated from the endothermic drift curves in the temperature-rating periods during the series of heat capacity measurements for the slowly precooled sample. Though the curves could not be well fitted in terms of an exponential function on account of the presence of a wide distribution of relaxation times, the function was used to estimate the order of magnitude for the relaxation time. A square and a triangle stand for the results evaluated in the same way from the exothermic drift curves, such as shown in Fig. 8(b), at 281 K and 252 K, respectively, immediately after rapid cooling from 330 K. All the points are located in the range of $10^3$–$10^5$ s. This is reasonable in view of the experimental feature that the present calorimetry tracks the relaxation in the time duration between $10^2$ s and $\sim 10^5$ s after each rapid temperature jump, and therefore one observes only the processes proceeding with the relaxation times between $10^2$ and $10^6$ s (or $10^7$ s in the case of very large enthalpy to relax), as stated in Sec. II. The relaxation time for the exothermic process appears to be longer than that for the endothermic one. This would be attributed primarily to the different distances, over which the excess oxygen ions diffuse in the respective processes, namely, to the magnitude of temperature jump, and secondarily to the different characters of the processes in the directions of increasing or decreasing the difference between the excess oxygen compositions of the two phases. The maximum number of jumps was tentatively estimated so as to include the relaxation time for the exothermic drift at 281 K: The straight line (b) represents the temperature dependence of the relaxation times expressed by Eq. (5) with $n = 10^7$. This indicates that the oxygen ions jump by $10^7$ times the order of magnitude when the phase separation newly occurs. It follows from the consideration of the random-walk problem that the oxygen ions effectively move by $10^3$–$10^4$ steps more or less in one direction. It is noticed that the two phases in the $La_2CuO_{4+\delta}$ crystal have been reported to be arranged in a period of a few hundreds Å,[21] which would correspond to the distance of a few hundred steps in the diffusion of oxygen. The number of steps estimated above is thus not inconsistent with the value expected from the structural data of related crystal $La_2CuO_{4+\delta}$.[21]

## V. CONCLUDING REMARKS

Phase separation with respect to the excess oxygen composition and the associated glass transition were observed in a $La_2NiO_{4.094}$ single crystal by calorimetry. The calorimetric appearance of a glass transition due to freezing-in of a phase separation process in the composition was found to differ very much in the temperature range of the anomaly from those of the glass transitions observed in macroscopically homogeneous systems.[15] A simple formulation model proposed for the characteristic time of the diffusion process was proved to be potentially well applied to evaluation of the relaxation times for phase separation processes such as the present sys-

tem. To what extent consideration of the random-walk problem holds for such phase separation processes should be examined in the future by using other techniques such as electron microscopy.

The characteristics of the spontaneous temperature drifts in the phase separation temperature region and the precooling-rate dependence of the drifts are suggestive of the $\delta$-$T$ phase relation for the $La_2CuO_{4+\delta}$ system with $0.01 < \delta < 0.04$. Two different interpretations have been given for the presence of two phases with different structures and the annealing effect on the production of the phases below room temperature:[9,10,22] One recognizes those observations as attributed to the phase separation just as in the $La_2NiO_{4.094}$ crystal,[22] and the other to the phase transitions of the first-order displacive type and/or of the Martensitic type.[9,10] The latter assumes that the phase separation concerning the oxygen composition proceeds above room temperature and that the compositions of the two regions in the sample do not change appreciably below room temperature. The present observation on $La_2NiO_{4.094}$ crystals, as well as the analogy of the $\delta$-$T$ phase diagram in $La_2NiO_{4+\delta}$ with $0.01 < \delta < 0.04$,[7,11,20] supports the latter of the two interpretations, since characteristic spontaneous heat evolution and absorption effects due to a glass transition have not been observed in $La_2CuO_{4+\delta}$ ($\delta = 0.011$ and 0.035) crystals.[9,10]

The temperature dependence of spontaneous heat evolution and absorption effects due to the phase separation in $La_2NiO_{4.094}$ crystals indicated that the excess oxygen compositions of at least one of the two phases changed even at 200 K. What $\delta$ values are energetically favored by the crystal structures of $La_2NiO_{4+\delta}$ at low temperatures is a subject still remaining to be clarified. The accumulated studies on the $\delta$-$T$ phase relation by calorimetry combined with diffractometry are expected to lead to a conclusion on the subject of interest.

## ACKNOWLEDGMENTS

This work was partly supported by a Grant-in-Aid for Scientific Research, the Ministry of Education, Science and Culture of Japan.

* Author to whom correspondence should be addressed.

[1] T. Kajitani, S. Hosoya, M. Hirabayashi, T. Fukuda, and T. Onozuka, J. Phys. Soc. Jpn. **58,** 3616 (1989).
[2] B. Dabrowski, J. D. Jorgensen, D. G. Hinks, S. Pei, D. R. Richards, H. B. Vanfleet, and D. L. Decker, Physica C **162-164,** 99 (1989).
[3] J. E. Schirber, B. Morosin, R. M. Merill, P. F. Hlava, E. L. Venturini, J. F. Kwak, P. J. Nigrey, R. J. Baughman, and D. S. Ginley, Physica C **152,** 121 (1988); G. Demazeau, F. Tresse, Th. Plante, B. Chevalier, J. Etourneau, C. Michel, M. Hervieu, B. Raveau, P. Lejay, A. Sulpice, and R. Tournier, *ibid.* **153-155,** 824 (1988).
[4] J. D. Jorgensen, B. Dabrowski, S. Pei, D. R. Richards, and D. G. Hinks, Phys. Rev. B **40,** 2187 (1989).
[5] C. Chaillout, J. Chenavas, S. W. Cheong, Z. Fisk, M. Marezio, B. Morosin, and J. E. Schirber, Physica C **170,** 87 (1990).
[6] Z. Hiroi, T. Obata, M. Takano, Y. Bando, Y. Takeda, and O. Yamamoto, Phys. Rev. B **41,** 11 665 (1990).
[7] J. M. Tranquada, Y. Kong, J. E. Lorenzo, D. J. Buttrey, D. E. Rice, and V. Sachan, Phys. Rev. B **50,** 6340 (1994).
[8] J. D. Jorgensen, B. Dabrowski, S. Pei, D. G. Hinks, and L. Soderholm, Phys. Rev. B **38,** 11 337 (1988); M. F. Hundley, J. D. Thompson, S-W. Cheng, and Z. Fisk, *ibid.* **41,** 4062 (1990); P. C. Hammel, A. P. Reyes, Z. Fisk, M. Takigawa, J. D. Thompson, R. H. Heffner, and S-W. Cheng, *ibid.* **42,** 6781 (1990); J.-S. Zhou, H. Chen, and J. B. Goodenough, *ibid.* **50,** 4168 (1994).
[9] M. Itoh, M. Oguni, T. Kyômen, H. Tamura, J. D. Yu, Y. Yanagida, Y. Inaguma, and T. Nakamura, Solid State Commun. **90,** 787 (1994).
[10] T. Kyômen, M. Oguni, M. Itoh, and J. D. Yu, Phys. Rev. B **51,** 3181 (1995).
[11] S. Hosoya, T. Omata, K. Yamada, and Y. Endoh, Physica C **202,** 188 (1992).
[12] D. E. Rice and D. J. Buttrey, J. Solid State Chem. **105,** 197, (1993).
[13] H. Tamura, A. Hayashi, and Y. Ueda, Physica C **216,** 83 (1993).
[14] H. Fujimori and M. Oguni, Solid State Commun. **94,** 157 (1995).
[15] H. Suga and S. Seki, Faraday Discuss. Roy. Soc. Chem. **69,** 221 (1980).
[16] P. G. Shewmon, *Diffusion in Solids* (McGraw-Hill, New York, 1963).
[17] K. Kitayama, J. Solid State Chem. **87,** 165 (1990).
[18] H. Fujimori and M. Oguni, J. Phys. Chem. Solids **54,** 271 (1993).
[19] G. Aeppli and J. Buttrey, Phys. Rev. Lett. **61,** 203 (1988).
[20] K. Yamada, T. Omata, K. Nakajima, Y. Endoh, and S. Hosoya, Physica C **221,** 355 (1994).
[21] J. Ryder, P. A. Midgley, R. Exley, R. J. Beynon, D. L. Yaters, L. Afalfiz, and J. A. Wilson, Physica C **173,** 9 (1991).
[22] R. K. Kremer, E. Sigmund, V. Hizhnyakov, F. Hentsch, A. Simon, K. A. Müller, and M. Mehring, Z. Phys. B **86,** 319 (1992); E. T. Ahrens, A. P. Reyes, P. C. Hammel, J. D. Thompson, P. C. Canfield, and Z. Fisk, Physica C **212,** 317 (1993); A. P. Reyes, E. T. Ahrens, P. C. Hammel, J. D. Thompson, P. C. Canfield, Z. Fisk, and R. H. Heffner, J. Appl. Phys. **73,** 6323 (1993); R. K. Kremer, V. Hizhnyakov, E. Sigmund, A. Simon, and K. A. Müller, Z. Phys. B **91,** 169 (1993).